Electric dipole polarizability in neutron-rich Sn isotopes as a probe of nuclear isovector properties

Z. Z. Li (李征征) ⓘ, Y. F. Niu (牛一斐) ⓘ,* and W. H. Long (龙文辉) ⓘ
School of Nuclear Science and Technology, Lanzhou University, Lanzhou 730000, China

The determination of nuclear symmetry energy and, in particular, its density dependence is a long-standing problem for the nuclear physics community. Previous studies have found that the product of electric dipole polarizability α_D and symmetry energy at saturation density J has a strong linear correlation with L, the slope parameter of symmetry energy. However, the current uncertainty of J hinders the precise constraint on L. We investigate the correlations between electric dipole polarizability α_D (or times symmetry energy at saturation density J) in Sn isotopes and the slope parameter of symmetry energy L using the quasiparticle random-phase approximation based on the Skyrme Hartree-Fock-Bogoliubov model. A strong linear correlation between α_D and L is found in neutron-rich Sn isotopes where pygmy dipole resonance (PDR) gives a considerable contribution to α_D, attributed to the pairing correlations playing important roles through PDR. This newly discovered linear correlation would help one to constrain L and neutron-skin thickness ΔR_{np} stiffly if α_D is measured with high resolution in neutron-rich nuclei. Additionally, a linear correlation between $\alpha_D J$ in a nucleus around the β-stability line and α_D in a neutron-rich nucleus can be used to assess α_D in neutron-rich nuclei.

I. INTRODUCTION

The determination of the nuclear equation of state (EoS) at high density is a challenge for both experimental and theoretical nuclear physics [1,2], which is crucial for constraining current theoretical models [3,4] and understanding many phenomena in astrophysics [5,6]. The biggest uncertainty of EoS comes from its isovector parts, which are governed by the nuclear symmetry energy $\mathcal{S}(\rho)$. The symmetry energy can be expanded as a function of $\varepsilon = (\rho - \rho_0)/3\rho_0$ by

$$\mathcal{S}(\rho) = J + L\varepsilon + \tfrac{1}{2}K_{\text{sym}}\varepsilon^2 + \dots \quad (1)$$

where $J = \mathcal{S}(\rho_0)$ is the symmetry energy at saturation density ρ_0, while $L = 3\rho_0(\frac{\partial \mathcal{S}}{\partial \rho})|_{\rho=\rho_0}$ and $K_{\text{sym}} = 9\rho_0^2(\frac{\partial^2 \mathcal{S}}{\partial \rho^2})|_{\rho=\rho_0}$ correspond to the slope and curvature parameters at saturation density, respectively.

The slope parameter of symmetry energy L determines the behavior of symmetry energy at high density; however, it varies a lot in different nuclear models. Constraints on L can be obtained from heavy-ion collisions [1,7], properties of neutron stars [5,8], and nuclear properties of ground and excited states of finite nuclei [9]. For example, it is revealed that L is proportional to the neutron-skin thickness ΔR_{np} by the droplet model [10,11], which is further confirmed by many microscopic models [12,13]. However, obstacles in the measurements of neutron radius hinder access to high-resolution neutron-skin data. As an alternative, charge radii difference ΔR_c between mirror nuclei is proposed as another possible way to constrain L [14–16], which also faces difficulties in the measurements of charge radius in a proton-rich nucleus.

The electric dipole ($E1$) excitation in a nucleus is mainly composed of giant dipole resonance (GDR), which is formed by the relative dipole oscillation between neutrons and protons, thus reflecting asymmetry information in nuclear EoS. The electric dipole polarizability α_D, being proportional to the inverse energy-weighted sum rule of $E1$ excitation, can serve as a possible probe for nuclear isovector properties. Theoretically, the (quasiparticle) random-phase approximation [(Q)RPA] approach is widely used to describe small oscillations of nuclei, such as $E1$ excitations. Self-consistent (Q)RPA models have been developed based on Skyrme density functionals [17–19], Gogny density functionals [20,21], and relativistic density functionals [22–25]. Global properties of GDR, such as centroid energies and electric dipole polarizabilities, can be well described within this approximation.

Based on these self-consistent (Q)RPA models, correlations between electric dipole polarizability α_D and other nuclear isovector properties have been investigated in recent years. Calculations performed by RPA model based on Skyrme density functionals in the SV-min series [26] and relativistic density functionals in the RMF-δ-t series in ^{208}Pb suggested a strong linear correlation between α_D and neutron-skin thickness ΔR_{np} [27]. However, when one combines the results from a host of different nuclear density functionals, this linear correlation is not universal anymore [28]. Starting from the droplet model, and further supported by RPA calculations based on many different Skyrme and relativistic density functionals in ^{208}Pb, the product of dipole polarizability and symmetry energy at saturation density $\alpha_D J$ was suggested to be much better correlated with neutron-skin thickness and symmetry energy slope parameter L than α_D alone is [29]. Based on this correlation, $L = 43 \pm (6)_{\text{expt}} \pm (8)_{\text{theor}} \pm (12)_{\text{est}}$ MeV was given by using the experimental α_D

*niuyf@lzu.edu.cn

value in ^{208}Pb [29], and the intervals $J = 30$–35 MeV and $L =$ 20–66 MeV were further obtained by combining the measured polarizabilities in ^{68}Ni, ^{120}Sn, and ^{208}Pb [30]. Below saturation density, α_D in ^{208}Pb was also found to be sensitive to both the symmetry energy $\mathcal{S}(\rho_c)$ and slope parameter $L(\rho_c)$ at the subsaturation cross density $\rho_c = 0.11$ fm^{-3} [31]. Since $\mathcal{S}(\rho_c)$ is well constrained, $L(\rho_c)$ can be strongly constrained from experimental α_D in ^{208}Pb [31]. At $\rho_r = \rho_0/3$, another linear correlation was built between α_D^{-1} and $\mathcal{S}(\rho_r)$ [32]. Additionally, α_D between two different nuclei [33], as well as $\alpha_D J$ between two different nuclei [30], were also shown to have good linear correlations.

In recent years, the electric dipole polarizabilities α_D in ^{208}Pb [34], ^{48}Ca [35], and stable Sn isotopes [33,36,37] were measured with high resolution via polarized proton inelastic scattering at extreme forward angles [38]. For unstable nucleus ^{68}Ni, α_D was also extracted by Coulomb excitation in inverse kinematics [39]. However, there are problems when one uses these high-resolution dipole polarizability data to constrain isovector properties: the constraint on L or ΔR_{np} is either with big uncertainties due to the uncertainty of J or with very big model uncertainties. One way to solve the problem and constrain L stiffly is to find a stronger and direct correlation between α_D and L. Although the previous studies have shown that the model-independent linear correlation only exists between $\alpha_D J$ and L, it was only limited to stable nuclei or nuclei near the β-stability line. It is well known that exotic phenomena will be present when approaching nuclei far from the β-stability line, such as novel shell structures [42–46], new types of excitations [23,47,48], and so on. Previous studies have shown that properties of neutron-rich nuclei with $N \approx 2Z$, such as binding energy, show stronger sensitivity to the symmetry energy parameters [40,41]. For $E1$ excitations, pygmy dipole resonance (PDR) appears in neutron-rich nuclei [23,47,48], which would cause different characteristics of $E1$ excitations compared to the ones around the β-stability line, and further affect α_D. So an interesting question is if the linear correlation between $\alpha_D J$ and L observed in stable nuclei still holds and new correlations would appear in neutron-rich nuclei.

Therefore, in our paper we will explore the correlations between α_D and nuclear isovector properties such as slope parameter L and neutron-skin thickness ΔR_{np} in even-even Sn isotopes from neutron-deficient ^{100}Sn to neutron-rich ^{164}Sn. The calculations are performed by QRPA based on the Skyrme Hartree-Fock-Bogoliubov (HFB) model, in which the spherical symmetries are imposed. The linear correlations are evaluated by a least-square regression analysis. Based on the newly discovered correlations, constraints on L and neutron-skin thickness will be discussed.

II. THEORETICAL FRAMEWORK

We carry out a self-consistent HFB + QRPA calculation of $E1$ strength using 24 Skyrme functionals: SIII, SIV, SV, SVI [49], SLy230a, SLy230b, SLy4, SLy5, SLy8 [50,51], SAMi [52], SAMi-J30, SAMi-J31, SAMi-J32, SAMi-J33 [53], SGI, SGII [54], SkM [55], SkM* [56], Ska [57], MSk1, MSk2 [58], MSk7 [59], BSk1 [60],

BSk2 [61]. The detailed formulas of QRPA on top of HFB can be found in Ref. [18]. The density-dependent zero-range surface pairing force is implemented in the particle-particle channel:

$$V_{pp}(\boldsymbol{r}_1, \boldsymbol{r}_2) = V_0 \left[1 - \frac{\rho(\boldsymbol{r})}{\rho_0} \right] \delta(\boldsymbol{r}_1 - \boldsymbol{r}_2) \quad (2)$$

where $\boldsymbol{r} = (\boldsymbol{r}_1 + \boldsymbol{r}_2)/2$, and $\rho_0 = 0.16$ fm^{-3} is the nuclear saturation density, while V_0 is adjusted by fitting neutron pairing gaps of $^{116\sim130}$Sn according to the five-point formula [62]. The electric dipole polarizability α_D is given by

$$\alpha_D = \frac{8\pi e^2}{9} m_{-1}, \quad m_{-1} = \sum_\nu \frac{\left| \langle \psi_\nu \| F_1^{(IV)} \| \psi_0 \rangle \right|^2}{E_\nu} \quad (3)$$

where ψ_ν and E_ν are the eigenstates and eigenvalues of QRPA equations, and ψ_0 is the ground state. m_{-1} is the inverse energy-weighted sum rule, which is calculated using the isovector dipole operator:

$$F_{1\mu}^{(IV)} = \frac{N}{A} \sum_{p=1}^Z r_p Y_{1\mu} - \frac{Z}{A} \sum_{n=1}^N r_n Y_{1\mu} \quad (4)$$

where A, N, and Z denote mass number, neutron number, and proton number, and $Y_{1\mu}$ are the spherical harmonics. In our calculations, the quasiparticle energy cutoff E_{cut} is set as 90 MeV and the total angular momentum cutoff of quasiparticle j_{max} is set as 21/2 to ensure the convergence of numerical results.

III. RESULTS AND DISCUSSIONS

A. Correlations between α_D and nuclear isovector properties

First of all, we study if the previously discovered linear correlation between $\alpha_D J$ and L holds in all tin isotopes from neutron-deficient ones to neutron-rich ones. So in Table I, Pearson correlation coefficients (or Pearson coefficient) r between $\alpha_D J$ and L in even-even Sn isotopes from ^{100}Sn to ^{160}Sn, as well as the corresponding slopes k of the regression lines, are shown based on the HFB+QRPA calculations using 24 Skyrme density functionals. Pearson coefficient r is a statistic that measures linear correlation between two variables, which is defined by the covariance of two variables divided by the product of their standard deviations. A value of $|r| = 1$ means that the two observables are fully linearly correlated while $r = 0$ means they are totally uncorrelated. From Table I, one can see the Pearson coefficients r in all Sn isotopes are all above 0.95, showing strong linear correlations between $\alpha_D J$ and L. So it further proves this linear correlation is a universal one which exists not only in stable nuclei as revealed in previous studies [29] but also in neutron-deficient and neutron-rich nuclei. The corresponding slope k of the regression line shows a clear increase trend with the increase of neutron number. The larger k value means a more rapid increase of $\alpha_D J$ as a function of L, which gives a smaller range of L under the same uncertainty of $\alpha_D J$. So the slope k of the regression line is an important quantity to select good candidate nuclei as probes of nuclear isovector properties, which will be discussed in detail in Sec. III B.

TABLE I. Pearson coefficient r between the product of dipole polarizability and saturated symmetry energy $\alpha_D J$ and the slope parameter of symmetry energy L in Sn isotopes, as well as the corresponding slope k of the regression line ($\alpha_D J$ as a function of L), calculated by QRPA based on HFB with 24 Skyrme density functionals.

Nucleus	^{100}Sn	^{110}Sn	^{120}Sn	^{130}Sn	^{140}Sn	^{150}Sn	^{160}Sn
r	0.975	0.977	0.981	0.971	0.975	0.967	0.951
k (fm^3)	0.837	1.071	1.361	1.503	2.234	2.837	3.406

Although the above correlation is universal, it cannot provide a stiff constraint on the slope parameter of symmetry energy L due to the uncertainty in the symmetry energy J. For example, by adopting $J = 31 \pm 2$ MeV, Roca-Maza *et al.* obtained $L = 43 \pm (6)_{\text{expt}} \pm (8)_{\text{theor}} \pm (12)_{\text{est}}$ MeV, where the uncertainty ± 12 MeV comes from the uncertainty of J [29]. So it would be better to find a direct correlation between α_D and L. Previous studies have shown that L and α_D have a good linear correlation within some specific parameter family [27]; however, by including different parameter families, this correlation becomes bad; for example, in ^{208}Pb the Pearson coefficient r was given as $r = 0.62$ [29] and $r = 0.77$ [28]. Here we recheck the correlation between the dipole polarizability α_D and the slope parameter L of symmetry energy for all tin isotopes from neutron-deficient ones to neutron-rich ones, as shown in Fig. 1, to see if the previous conclusions still hold. In stable nucleus ^{120}Sn, for some specific Skyrme parameter family, such as SAMi (green diamonds) or SIII-SVI (up blue triangles), one can observe a good linear correlation, in agreement with Ref. [27]. However, when one includes more different Skyrme parameter sets, the linear correlation becomes poor, and the Pearson coefficient r is around 0.85, again in agreement with the case in ^{208}Pb [28,29]. Similar situations still exist in nuclei not far from the stability line such as ^{100,110,130}Sn.

However, the cases become totally different in the neutron-rich nuclei. The coefficients are above 0.9 for the isotopes with mass number $A \geqslant 136$, which present strong correlations between α_D and L in the neutron-rich Sn isotopes. After $A \geqslant 146$, where the neutron number is nearly equal to twice the proton number, the correlation between α_D and L is even better than the one between $\alpha_D J$ and L. We stress here that the assessments are carried out by a variety of different Skyrme functional families. However, it needs to be further checked by the inclusion of more nuclear models. For the neutron-rich nuclei of $A \geqslant 136$ with a clear linear correlation, we further give the slopes k of the regression lines. It is seen that k becomes larger with the increase of neutron number, which implies that the more neutron rich the nucleus is, the better the probe it can serve as for nuclear isovector properties. This result also supports the previous findings in Ref. [41] that the properties of extreme neutron-rich systems play a predominant role in narrowing down the uncertainties in the various symmetry energy parameters.

To understand the above strong linear correlations in neutron-rich Sn isotopes, we first investigate the role of pairing correlations. So in Fig. 2 the correlations between α_D and L in ^{120,140,150,160}Sn are studied without considering pairing effects. For stable nucleus ^{120}Sn, the correlation between α_D and L is similar to the case with pairing correlations, where
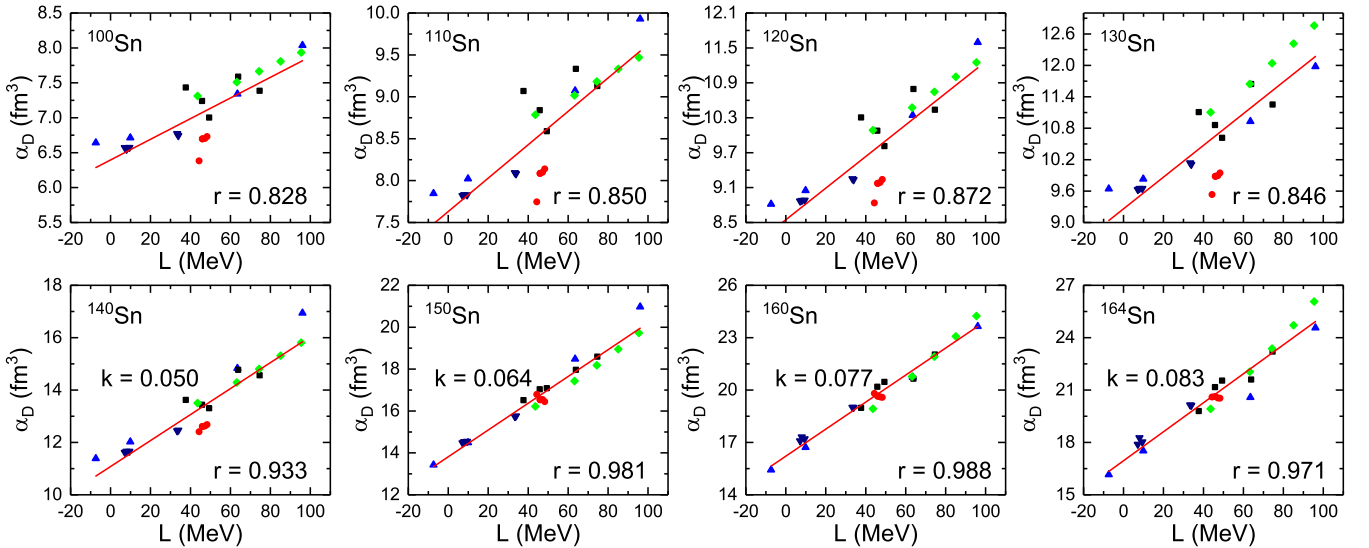

FIG. 1. Plots for dipole polarizability α_D against slope parameter of symmetry energy L in Sn isotopes calculated by QRPA based on HFB with 24 Skyrme density functionals: SIII, SIV, SV, SVI (blue up triangles); SLy230a, SLy230b, SLy4, SLy5, SLy8 (red circles); SAMi, SAMi-J30, SAMi-J31, SAMi-J32, SAMi-J33 (green diamonds); SGI, SGII, SkM, SkM*, Ska (black squares); MSk1, MSk2, MSk7, BSk1, BSk2 (navy blue down triangles). A regression line (red solid line) is obtained by a least-square linear fit of the calculated α_D as a function of L. r is Pearson coefficient and k (fm^3/MeV) is the slope of the regression line.
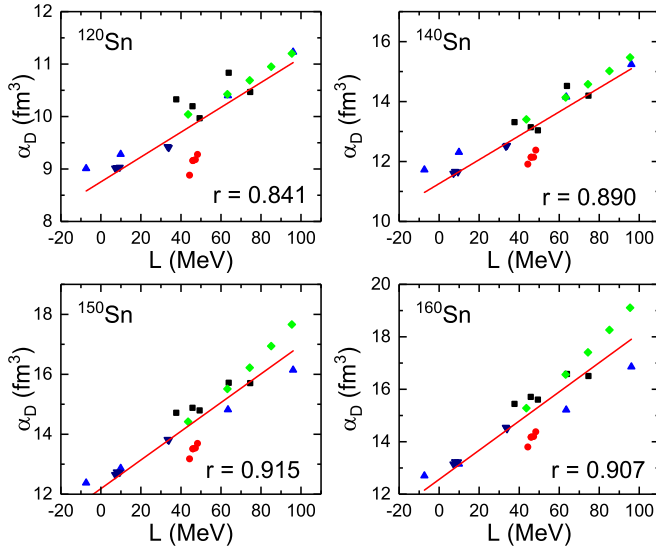
FIG. 2. The same as Fig. 1 but for ^{120,140,150,160}Sn without the pairing correlations.
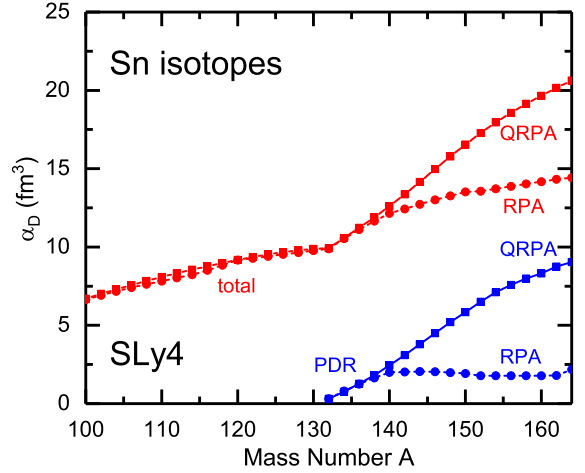

FIG. 3. The dipole polarizabilities as functions of mass number A in even-even Sn isotopes calculated by QRPA (square line) and RPA (circle line) using Skyrme functional SLy4. The total dipole polarizabilities (red) and the contributions from PDR (blue) are shown, respectively.

the Pearson coefficient is only slightly reduced without the inclusion of pairing correlations. Going towards neutron-rich nucleus ^{140}Sn, the linear correlation coefficient reduces more. For more neutron-rich nuclei ^{150,160}Sn, the linear correlations become much worse, where the Pearson coefficients are largely reduced to the values 0.915 and 0.917, respectively. This shows that the pairing correlations play important roles in keeping strong linear correlations between α_D and L in neutron-rich Sn isotopes.

On the other hand, for neutron-rich nuclei, the PDR appears in the low-energy part of the $E1$ transition strength distribution, which would give big contributions to the dipole polarizability. Since PDR represents an oscillation between the neutron skin and the nearly isospin-saturated core, the correlations between its strengths and symmetry energy were also explored [27,63–65], although it is still an open question. Inspired by this, we extract the contributions of PDR to α_D in Sn isotopes in Fig. 3, where the total dipole polarizabilities and contributions from PDR as functions of mass number A in even-even Sn isotopes calculated by QRPA and RPA using Skyrme functional SLy4 are plotted. According to the dipole strength distributions and the transition densities, different energies are selected as the upper boundaries of PDR for different Skyrme functionals, which are 8.5 MeV for MSk and BSk families; 9.0 MeV for SVI; 10.0 MeV for SIII, the SLy family, SkM, SkM*, and SGII; 10.5 MeV for Ska and the SAMi family; 11.0 MeV for SGI; 12.0 MeV for SIV; and 13.0 MeV for SV.

Starting from ^{132}Sn, the PDR appears and starts to contribute to the dipole polarizability α_D. When the neutron number increases, the contribution from PDR becomes larger and larger, which dominates the evolution trend with mass number of the total α_D. With the pairing correlations being turned off, the contribution from PDR to α_D is greatly reduced, which almost keeps a small constant with the increase of neutron number. As a result, the total α_D is also reduced a

lot, and its increase trend with mass number becomes as slow as that before ^{132}Sn. Before ^{132}Sn, the pairing correlations only have very small influences on α_D. Therefore, it can be seen that the pairing correlations play their important roles on dipole polarizabilities and further the linear correlations between α_D and L through PDR.

In Fig. 4 we further study the correlation between dipole polarizabilities α_D contributed by PDR and the slope parameter L of symmetry energy in ^{134}Sn, ^{140}Sn, ^{150}Sn, and ^{160}Sn isotopes. It shows that polarizability α_D of PDR has a good correlation with the slope parameter L in general,
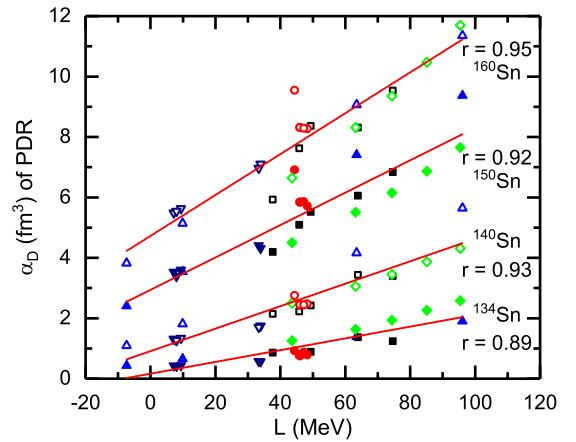

FIG. 4. Plots for dipole polarizability contributed by PDR against slope parameter of symmetry energy in ^{134,140,150,160}Sn isotopes calculated by QRPA based on HFB with 24 Skyrme density functionals: SIII, SIV, SV, SVI (blue up triangles); SLy230a, SLy230b, SLy4, SLy5, SLy8 (red circles); SAMi, SAMi-J30, SAMi-J31, SAMi-J32, SAMi-J33 (green diamonds); SGI, SGII, SkM, SkM*, Ska (black squares); MSk1, MSk2, MSk7, BSk1, BSk2 (navy blue down triangles). A linear fit is done for each nucleus (red solid line) with a corresponding Pearson coefficient r.
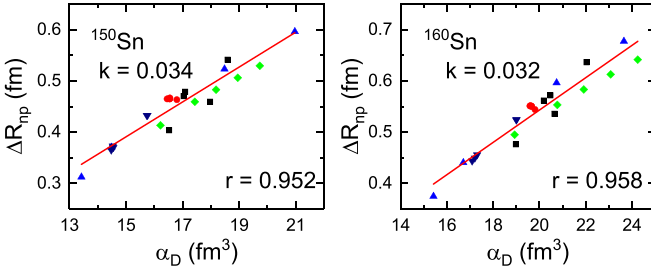
FIG. 5. Plots for neutron-skin thickness ΔR_{np} against dipole polarizability α_D in ^{150,160}Sn calculated by QRPA based on HFB with 24 Skyrme density functionals: SIII, SIV, SV, SVI (blue up triangles); SLy230a, SLy230b, SLy4, SLy5, SLy8 (red circles); SAMi, SAMi-J30, SAMi-J31, SAMi-J32, SAMi-J33 (green diamonds); SGI, SGII, SkM, SkM*, Ska (black squares); MSk1, MSk2, MSk7, BSk1, BSk2 (navy blue down triangles). A regression line (red solid line) is obtained by a least-square linear fit of the calculated ΔR_{np} as a function of α_D. r is Pearson coefficient and k (fm^{-2}) is the slope of regression line.

which enhances the linear correlations between the total α_D and symmetry energy slope parameter L.

Apart from the correlation between α_D and L, the correlation between α_D and another important isovector property, i.e., neutron-skin thickness, is also investigated, and the plots for neutron-skin thickness against dipole polarizability in ^{150,160}Sn are shown in Fig. 5. Not surprisingly, the linear correlations between ΔR_{np} and α_D in ^{150}Sn and ^{160}Sn are strong with $r = 0.952$ and 0.958, respectively, since the neutron-skin thickness ΔR_{np} and L are reported to have a good linear correlation when $|N - Z|$ is large [15]. The slopes k of regression lines, fitted by ΔR_{np} as a function of α_D, are generally small in these neutron-rich nuclei, suggesting that α_D in neutron-rich nuclei can provide an effective constraint on neutron-skin thickness of the corresponding nuclei.

B. α_D as a probe of nuclear isovector properties

In Sec. III A, the correlations between α_D (or $\alpha_D J$) and nuclear isovector properties, e.g., L and ΔR_{np}, are investigated for all tin isotopes, so in the following we will analyze what information we can obtain from these correlations, and which

nucleus could be treated as a proper probe of nuclear isovector properties in terms of dipole polarizabilities.

Experimentally, the dipole polarizabilities of ^{208}Pb [34], ^{68}Ni [39], ^{48}Ca [35], and stable Sn isotopes [36] were measured with high resolution. The correlations between $\alpha_D J$ and L are always strong for both stable nuclei and nuclei far from the stability line from previous studies and our results in Sec. III A. So in Table II we show the constraints on the slope parameter of symmetry energy L from experimental dipole polarizability values $\alpha_D^{exp.}$ using correlation between $\alpha_D J$ and L in these experimentally measured nuclei. The correlations between $\alpha_D J$ and L are obtained by QRPA calculations using 24 Skyrme density functionals as done in Sec. III A. The corresponding Pearson coefficients r and slopes k of regression lines fitted by $\alpha_D J$ as a function of L are also given in Table II. It can be seen that the linear correlations are well kept for all these nuclei with $r > 0.95$. $J = 31.7 \pm 3.2$ MeV from the statistic analysis of various available constraints [2] is adopted for deducing the L value. The uncertainty of L is determined by $\Delta L = (J \Delta \alpha_D + \alpha_D \Delta J)/k$, where $\Delta \alpha_D$ and ΔJ are the uncertainties of α_D and J, respectively. From Table II, it can be seen that L has remarkable uncertainties which are all larger than ± 30 MeV. In the limiting case $\Delta \alpha_D = 0$, the uncertainty of slope parameter ΔL_{min} comes only from the uncertainty of J, which is also given in Table II, which shows that the uncertainty of J contributes more than half of the total uncertainties of L, which hinders the effective constraints on L from the correlation between $\alpha_D J$ and L. However, with the increase of neutron number in Sn isotopes, ΔL_{min} has the tendency to become smaller. This is because the slope k of the regression line increases faster than the dipole polarizability α_D with the increase of neutron number, and hence α_D/k becomes smaller. So the uncertainty caused by ΔJ would become small if one finds a nucleus with a small α_D/k value.

Based on the analysis of neutron-rich Sn isotopes with 24 Skyrme functionals in Sec. III A, a strong correlation between α_D and L appears in neutron-rich nuclei (seeing Fig. 1) where the PDR gives a considerable contribution to the inverse energy-weighted sum rule m_{-1}. So it provides a more effective way to constrain L directly from dipole polarizability. Moreover, the slope k of the regression line (in Fig. 1) becomes larger with the increase of neutron number, which makes the

TABLE II. Constraints on the slope parameter of symmetry energy L from experimental dipole polarizability values $\alpha_D^{exp.}$ [30,34–36,39] using linear correlation between $\alpha_D J$ and L obtained by Skyrme QRPA calculations using 24 Skyrme functionals. The Pearson coefficient r and the slope k of the regression line fitted by $\alpha_D J$ as a function of L are also given. $J = 31.7 \pm 3.2$ MeV is adopted [2]. ΔL_{min} denotes the uncertainty coming from the uncertainty of J.

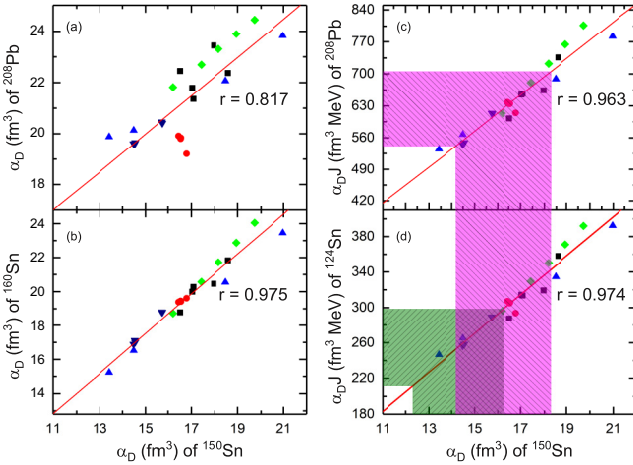| Nucleus	$\alpha_D^{exp.}$ (fm^3)	r	k (fm^3)	L (MeV)	ΔL_{min} (MeV)
^{208}Pb	19.6 ± 0.60	0.98	2.632	38.07 ± 31.05	± 23.83
^{68}Ni	3.88 ± 0.31	0.97	0.554	33.29 ± 40.16	± 22.42
^{48}Ca	2.07 ± 0.22	0.97	0.323	15.76 ± 42.11	± 20.51
^{112}Sn	7.19 ± 0.50	0.98	1.106	12.81 ± 35.13	± 20.80
^{114}Sn	7.29 ± 0.58	0.98	1.154	10.62 ± 36.16	± 20.22
^{116}Sn	7.52 ± 0.51	0.98	1.225	12.03 ± 32.85	± 19.64
^{118}Sn	7.91 ± 0.87	0.98	1.299	18.44 ± 40.72	± 19.49
^{120}Sn	8.08 ± 0.60	0.98	1.362	17.67 ± 32.98	± 19.00
^{124}Sn	7.99 ± 0.56	0.98	1.439	8.46 ± 30.10	± 17.77

FIG. 6. The dipole polarizability α_D (a) in ^{208}Pb and (b) in ^{160}Sn as a function of the dipole polarizability in ^{150}Sn. The dipole polarizability α_D (c) in ^{208}Pb and (d) in ^{124}Sn times the symmetry energy at saturation density J as a function of the dipole polarizability in ^{150}Sn. Calculations are done by QRPA based on HFB with 24 Skyrme density functionals: SIII, SIV, SV, SVI (blue up triangles); SLy230a, SLy230b, SLy4, SLy5, SLy8 (red circles); SAMi, SAMi-J30, SAMi-J31, SAMi-J32, SAMi-J33 (green diamonds); SGI, SGII, SkM, SkM*, Ska (black squares); MSk1, MSk2, MSk7, BSk1, BSk2 (navy blue down triangles). r is the Pearson coefficient. Utilizing the experimental values of α_D in ^{208}Pb [30,34] and in ^{124}Sn [36], and assuming $J = 31.7 \pm 3.2$ MeV [2], the dipole polarizability of ^{150}Sn is predicted to be between 14.18 and 16.27 fm^3.

constraints on L from this correlation in neutron-rich nuclei more stiff. For example, an uncertainty of ± 0.5 fm^3 in α_D of ^{140}Sn, which is about the present accuracy for experimental measurement in dipole polarizability, could constrain L within ± 10 MeV, while with the same uncertainty of α_D in ^{160}Sn, L can be constrained within ± 6.5 MeV. However, for these neutron-rich nuclei, the experimental data for dipole polarizabilities are still unavailable, so we first need to make predictions on α_D in neutron-rich nuclei.

In Fig. 6(a), we study the correlations of α_D between ^{208}Pb and ^{150}Sn. Although it was found that α_D between two stable nuclei, e.g., between ^{208}Pb and ^{120}Sn, have a good linear correlation [30,33]; this correlation is no longer well kept when it is extended to α_D between one stable nucleus and one neutron-rich nucleus, e.g., between ^{208}Pb and ^{150}Sn, as seen in Fig. 6(a). The correlation between two neutron-rich nuclei, e.g., between ^{160}Sn and ^{150}Sn, is further checked in Fig. 6(b), and it becomes strong again. So one fails to predict α_D of neutron-rich nuclei from α_D of stable nuclei directly. Since both $\alpha_D J$ in stable nuclei and α_D in neutron-rich nuclei linearly correlate with L, $\alpha_D J$ in stable nuclei should also linearly correlate with α_D in neutron-rich nuclei. This is checked by our calculations in Fig. 6, where $\alpha_D J$ in ^{208}Pb [Fig. 6(c)] and in ^{124}Sn [Fig. 6(d)] as a function of α_D in ^{150}Sn are plotted. Good linear correlations with $r = 0.963$ and 0.974 are found, respectively, which can be used for the predictions of α_D in ^{150}Sn as well as other neutron-rich nuclei. Utilizing the experimental α_D values of ^{208}Pb and ^{124}Sn, shown in Table II,

and adopting $J = 31.7 \pm 3.2$ MeV [2], $\alpha_D \in [12.31, 16.27]$ and $[14.18, 18.28]$ fm^3 are obtained for ^{150}Sn. The overlap $\alpha_D \in [14.18, 16.27]$ fm^3 is finally taken as the predicted value for ^{150}Sn.

The same process can be done for other neutron-rich nuclei. The predicted α_D from ^{140}Sn to ^{160}Sn are given in Table III, with which the corresponding constraints on L and neutron-skin thickness ΔR_{np} are deduced and presented in Table III from the correlations between α_D and L, as well as between ΔR_{np} and α_D. The corresponding Pearson coefficients r of both correlations are shown in Table III, and it can be seen that the linear correlations are very well kept for all these neutron-rich nuclei. Here since the L values are constrained from the linear correlation between α_D and L directly, the uncertainties become much smaller compared to those shown in Table II. With the increase of neutron number, the slope of the regression line fitted by α_D as a function of L becomes larger, and as a result the uncertainty of L also becomes smaller until ^{156}Sn even with an increasing uncertainty in the predicted α_D^P. For the neutron-skin thickness, the slope of the regression line fitted by ΔR_{np} as a function of α_D keeps almost constant with increasing neutron number, yet the uncertainties of constrained neutron-skin thickness become larger due to the increasing uncertainties in α_D^P.

Making use of the direct correlations between α_D and L, small uncertainties in the value of L can be obtained, if the α_D values of neutron-rich nuclei can be measured with the same accuracy as the stable nuclei. However, since the correlations between α_D and L are studied within Skyrme density functionals, the uncertainties may become bigger with the introduction of different theoretical models. Due to the lack of experimental data of α_D in neutron-rich nuclei, the present constraints on L shown in Table III in fact do not give new information compared to the L values obtained from the correlation between L and $\alpha_D J$ in ^{208}Pb and in ^{124}Sn. Nevertheless, the direct correlation between α_D and L would show its special importance and effectiveness in constraining nuclear isovector properties when the experimental data of α_D in neutron-rich tin isotopes are available, so measurements of dipole polarizability towards neutron-rich nuclei are strongly called for.

IV. SUMMARY

The correlations between electric dipole polarizability α_D (or times symmetry energy at saturation density J) and slope parameter of symmetry energy L are studied in Sn isotopes preformed by QRPA based on Skyrme HFB theory. The previously found correlation between $\alpha_D J$ and L is confirmed in all Sn isotopes from neutron-deficient ones to neutron-rich ones. The linear correlation between α_D and L is not strong in stable tin isotopes and their surroundings; however, it becomes better for mass number $A > 132$, and strong correlations are found when $A \geqslant 136$ with the correlation coefficients $r > 0.9$, where PDR gives a considerable contribution to α_D. After $A \geqslant 146$, where the neutron number is nearly equal to twice the proton number, the correlation between α_D and L is even better than the one between $\alpha_D J$ and L. The enhancement of

TABLE III. Predictions of the dipole polarizabilities in neutron-rich Sn isotopes from experimental dipole polarizabilities of ^{208}Pb [30,34] and ^{124}Sn [36,37] using the correlations shown in Figs. 6(c) and 6(d). The constrained values of slope parameter of symmetry energy L and neutron-skin thickness of neutron-rich Sn isotopes are also given from the correlations shown in Figs. 1 and 5. The Pearson coefficients r and slopes of regression line k fitted by dipole polarizability α_D as a function of L, as well as by neutron-skin thickness ΔR_{np} as a function of α_D, are also shown, respectively.

Nucleus	α_D^P (fm^3)	α_D as a function of L			ΔR_{np} as a function of α_D		
		r	k (fm^3/MeV)	L (MeV)	r	k (fm^{-2})	ΔR_{np}(fm)
^{140}Sn	12.07 ± 0.88	0.93	0.050	19.9 ± 17.7	0.91	0.034	0.295 ± 0.030
^{142}Sn	12.67 ± 0.93	0.94	0.053	20.4 ± 17.4	0.92	0.034	0.317 ± 0.031
^{144}Sn	13.31 ± 0.96	0.96	0.056	20.9 ± 17.1	0.93	0.034	0.338 ± 0.033
^{146}Sn	13.95 ± 1.00	0.97	0.059	21.3 ± 16.8	0.94	0.034	0.359 ± 0.034
^{148}Sn	14.59 ± 1.02	0.97	0.062	21.7 ± 16.5	0.95	0.034	0.379 ± 0.035
^{150}Sn	15.22 ± 1.04	0.98	0.064	22.0 ± 16.3	0.95	0.034	0.398 ± 0.036
^{152}Sn	15.83 ± 1.07	0.99	0.066	22.3 ± 16.1	0.95	0.034	0.417 ± 0.036
^{154}Sn	16.41 ± 1.10	0.99	0.069	22.5 ± 16.0	0.96	0.033	0.434 ± 0.037
^{156}Sn	16.94 ± 1.13	0.99	0.071	22.7 ± 15.8	0.95	0.033	0.451 ± 0.037
^{158}Sn	17.48 ± 1.18	0.99	0.074	22.6 ± 15.9	0.96	0.032	0.465 ± 0.038
^{160}Sn	17.96 ± 1.23	0.99	0.077	22.6 ± 15.9	0.96	0.032	0.479 ± 0.039

this correlation between α_D and L is attributed to the pairing correlations, which play important roles through PDR.

With the available high-resolution data of α_D, the constraints on L are obtained from the correlation between $\alpha_D J$ and L. Large uncertainties of L are found, where more than half are contributed by the uncertainty from symmetry energy $\Delta J = \pm 3.2$ MeV. A proper candidate nucleus for constraining L is the one with a small α_D/k value, where k is the slope of the regression line fitted by $\alpha_D J$ as a function of L. In stable Sn isotopes, the α_D/k becomes smaller towards the neutron-rich side.

With the strong correlation between α_D and L in neutron-rich Sn isotopes, L can be constrained directly and more stiffly if experimental data of α_D with high resolution in these nuclei are known. At the moment, α_D in neutron-rich nuclei are predicted using the linear correlation between $\alpha_D J$ in a stable nucleus with experimental data and α_D in a neutron-rich nucleus.

The constraints on nuclear isovector properties are obtained based on the strong correlations between α_D and nuclear isovector properties in neutron-rich nuclei. Nevertheless, present calculations are still limited to Skyrme density functionals. More verifications of these correlations between α_D in neutron-rich nuclei and nuclear isovector properties based on different theoretical models are encouraged. At the same time, measurements of electric dipole polarizability towards neutron-rich nuclei are called for.

[1] B.-A. Li, L.-W. Chen, and C. M. Ko, Phys. Rep. **464**, 113 (2008).

[2] M. Oertel, M. Hempel, T. Klähn, and S. Typel, Rev. Mod. Phys. **89**, 015007 (2017).

[3] M. Dutra, O. Lourenço, J. S. Sá Martins, A. Delfino, J. R. Stone, and P. D. Stevenson, Phys. Rev. C **85**, 035201 (2012).

[4] M. Dutra, O. Lourenço, S. S. Avancini, B. V. Carlson, A. Delfino, D. P. Menezes, C. Providência, S. Typel, and J. R. Stone, Phys. Rev. C **90**, 055203 (2014).

[5] J. M. Lattimer and M. Prakash, Astrophys. J. **550**, 426 (2001).

[6] Z. W. Liu, Z. Qian, R. Y. Xing, J. R. Niu, and B. Y. Sun, Phys. Rev. C **97**, 025801 (2018).

[7] M. B. Tsang, Y. Zhang, P. Danielewicz, M. Famiano, Z. Li, W. G. Lynch, and A. W. Steiner, Phys. Rev. Lett. **102**, 122701 (2009).

[8] J. M. Lattimer and M. Prakash, Phys. Rep. **621**, 127 (2016).

[9] X. Roca-Maza and N. Paar, Prog. Part. Nucl. Phys. **101**, 96 (2018).

[10] W. D. Myers and W. J. Swiatecki, Nucl. Phys. A **336**, 267 (1980).

[11] M. Warda, X. Viñas, X. Roca-Maza, and M. Centelles, Phys. Rev. C **80**, 024316 (2009).

[12] B. A. Brown, Phys. Rev. Lett. **85**, 5296 (2000).

[13] L.-W. Chen, C. M. Ko, and B.-A. Li, Phys. Rev. C **72**, 064309 (2005).

[14] N. Wang and T. Li, Phys. Rev. C **88**, 011301(R) (2013).

[15] B. A. Brown, Phys. Rev. Lett. **119**, 122502 (2017).

[16] J. Yang and J. Piekarewicz, Phys. Rev. C **97**, 014314 (2018).

[17] G. Colò, L. Cao, N. Van Giai, and L. Capelli, Comp. Phys. Comm. **184**, 142 (2013).

[18] J. Terasaki, J. Engel, M. Bender, J. Dobaczewski, W. Nazarewicz, and M. Stoitsov, Phys. Rev. C **71**, 034310 (2005).

[19] E. Khan and N. Van Giai, Phys. Lett. B **472**, 253 (2000).

[20] G. Giambrone, S. Scheit, F. Barranco, P. F. Bortignon, G. Colò, D. Sarchi, and E. Vigezzi, Nucl. Phys. A **726**, 3 (2003).

[21] M. Martini, S. Péru, and M. Dupuis, Phys. Rev. C **83**, 034309 (2011).

[22] N. Paar, P. Ring, T. Nikšić, and D. Vretenar, Phys. Rev. C **67**, 034312 (2003).

[23] N. Paar, D. Vretenar, E. Khan, and G. Colò, Rep. Prog. Phys. **70**, 691 (2007).

[24] P. Ring, Z.-Y. Ma, N. Van Giai, D. Vretenar, A. Wandelt, and L.-G. Cao, Nucl. Phys. A **694**, 249 (2001).

[25] T. Nikšić, D. Vretenar, and P. Ring, Phys. Rev. C **66**, 064302 (2002).

[26] P. Klüpfel, P.-G. Reinhard, T. J. Bürvenich, and J. A. Maruhn, Phys. Rev. C **79**, 034310 (2009).

[27] P.-G. Reinhard and W. Nazarewicz, Phys. Rev. C **81**, 051303(R) (2010).

[28] J. Piekarewicz, B. K. Agrawal, G. Colò, W. Nazarewicz, N. Paar, P.-G. Reinhard, X. Roca-Maza, and D. Vretenar, Phys. Rev. C **85**, 041302(R) (2012).

[29] X. Roca-Maza, M. Brenna, G. Colò, M. Centelles, X. Viñas, B. K. Agrawal, N. Paar, D. Vretenar, and J. Piekarewicz, Phys. Rev. C **88**, 024316 (2013).

[30] X. Roca-Maza, X. Viñas, M. Centelles, B. K. Agrawal, G. Colò, N. Paar, J. Piekarewicz, and D. Vretenar, Phys. Rev. C **92**, 064304 (2015).

[31] Z. Zhang and L.-W. Chen, Phys. Rev. C **90**, 064317 (2014).

[32] Z. Zhang and L.-W. Chen, Phys. Rev. C **92**, 031301(R) (2015).

[33] T. Hashimoto, A. M. Krumbholz, P.-G. Reinhard, A. Tamii, P. von Neumann-Cosel, T. Adachi, N. Aoi, C. A. Bertulani, H. Fujita, Y. Fujita *et al.*, Phys. Rev. C **92**, 031305(R) (2015).

[34] A. Tamii, I. Poltoratska, P. von Neumann-Cosel, Y. Fujita, T. Adachi, C. A. Bertulani, J. Carter, M. Dozono, H. Fujita, K. Fujita *et al.*, Phys. Rev. Lett. **107**, 062502 (2011).

[35] J. Birkhan, M. Miorelli, S. Bacca, S. Bassauer, C. A. Bertulani, G. Hagen, H. Matsubara, P. von Neumann-Cosel, T. Papenbrock, N. Pietralla *et al.*, Phys. Rev. Lett. **118**, 252501 (2017).

[36] S. Bassauer, P. von Neumann-Cosel, P.-G. Reinhard, A. Tamii, S. Adachi, C. A. Bertulani, P. Y. Chan, A. D'Alessio, H. Fujioka, H. Fujita *et al.*, Phys. Rev. C **102**, 034327 (2020).

[37] S. Bassauer, P. von Neumann-Cosel, P.-G. Reinhard, A. Tamii, S. Adachi, C. A. Bertulani, P. Chan, G. Colò, A. D'Alessio, H. Fujioka *et al.*, Phys. Lett. B **810**, 135804 (2020).

[38] P. von Neumann-Cosel and A. Tamii, Eur. Phys. J. A **55**, 110 (2019).

[39] D. M. Rossi, P. Adrich, F. Aksouh, H. Alvarez-Pol, T. Aumann, J. Benlliure, M. Böhmer, K. Boretzky, E. Casarejos, M. Chartier *et al.*, Phys. Rev. Lett. **111**, 242503 (2013).

[40] C. Mondal, B. K. Agrawal, and J. N. De, Phys. Rev. C **92**, 024302 (2015).

[41] C. Mondal, B. K. Agrawal, J. N. De, and S. K. Samaddar, Phys. Rev. C **93**, 044328 (2016).

[42] F. Wienholtz, D. Beck, K. Blaum, C. Borgmann, M. Breitenfeldt, R. B. Cakirli, S. George, F. Herfurth, J. D. Holt, M. Kowalska *et al.*, Nature (London) **498**, 346 (2013).

[43] J. Liu, Y. F. Niu, and W. H. Long, Phys. Lett. B **806**, 135524 (2020).

[44] J. J. Li, W. H. Long, J. Margueron, and N. Van Giai, Phys. Lett. B **788**, 192 (2019).

[45] Z.-Z. Li, S.-Y. Chang, Q. Zhao, W.-H. Long, and Y.-F. Niu, Chin. Phys. C **43**, 074107 (2019).

[46] M. Grasso, Phys. Rev. C **89**, 034316 (2014).

[47] D. Savran, T. Aumann, and A. Zilges, Prog. Part. Nucl. Phys. **70**, 210 (2013).

[48] T. Aumann, Eur. Phys. J. A **55**, 234 (2019).

[49] M. Beiner, H. Flocard, N. Van Giai, and P. Quentin, Nucl. Phys. A **238**, 29 (1975).

[50] E. Chabanat, P. Bonche, P. Haensel, J. Meyer, and R. Schaeffer, Nucl. Phys. A **627**, 710 (1997).

[51] E. Chabanat, P. Bonche, P. Haensel, J. Meyer, and R. Schaeffer, Nucl. Phys. A **635**, 231 (1998).

[52] X. Roca-Maza, G. Colò, and H. Sagawa, Phys. Rev. C **86**, 031306(R) (2012).

[53] X. Roca-Maza, M. Brenna, B. K. Agrawal, P. F. Bortignon, G. Colò, L.-G. Cao, N. Paar, and D. Vretenar, Phys. Rev. C **87**, 034301 (2013).

[54] N. Van Giai and H. Sagawa, Phys. Lett. B **106**, 379 (1981).

[55] H. Krivine, J. Treiner, and O. Bohigas, Nucl. Phys. A **336**, 155 (1980).

[56] J. Bartel, P. Quentin, M. Brack, C. Guet, and H.-B. Håkansson, Nucl. Phys. A **386**, 79 (1982).

[57] H. S. Köhler, Nucl. Phys. A **258**, 301 (1976).

[58] F. Tondeur, S. Goriely, J. M. Pearson, and M. Onsi, Phys. Rev. C **62**, 024308 (2000).

[59] S. Goriely, F. Tondeur, and J. Pearson, Atomic Data and Nuclear Data Tables **77**, 311 (2001).

[60] M. Samyn, S. Goriely, P.-H. Heenen, J. Pearson, and F. Tondeur, Nucl. Phys. A **700**, 142 (2002).

[61] S. Goriely, M. Samyn, P.-H. Heenen, J. M. Pearson, and F. Tondeur, Phys. Rev. C **66**, 024326 (2002).

[62] M. Bender, K. Rutz, P.-G. Reinhard, and J. A. Maruhn, Eur. Phys. J. A **8**, 59 (2000).

[63] J. Piekarewicz, Phys. Rev. C **73**, 044325 (2006).

[64] A. Carbone, G. Colò, A. Bracco, L.-G. Cao, P. F. Bortignon, F. Camera, and O. Wieland, Phys. Rev. C **81**, 041301(R) (2010).

[65] D. Vretenar, Y. F. Niu, N. Paar, and J. Meng, Phys. Rev. C **85**, 044317 (2012).